Immature monocytes acquire antigens from other cells in the bone marrow and present them to T cells after maturing in the periphery

Frank Tacke,[1] Florent Ginhoux,[1] Claudia Jakubzick,[1] Nico van Rooijen,[2] Miriam Merad,[1] and Gwendalyn J. Randolph[1]

[1]Department of Gene and Cell Medicine, Icahn Research Institute, Mount Sinai School of Medicine, New York, NY 10029
[2]Department of Molecular Cell Biology, Free University Medical Center, 1081 HV Amsterdam, Netherlands

Monocytes are circulating precursors for tissue macrophages and dendritic cells (DCs) but are not recognized to directly participate in antigen presentation. We developed techniques to label mouse monocyte subsets with particulate tracers in vivo. Gr-1^{lo} but not Gr-1^{hi} monocytes were stably labeled by intravenous injection of 0.5-μm microspheres. Gr-1^{hi} monocytes could be labeled when the microspheres were injected after systemic depletion of blood monocytes and spleen macrophages. In this condition, the phagocytic tracer was transferred to immature bone marrow monocytes by neutrophils and B cells that first carried the particles to the bone marrow. Moreover, antigens from B cells or proteins conjugated to the tracer particles were processed for presentation by monocytes and could induce T cell responses in the periphery. Cell-associated antigen taken up by bone marrow monocytes was retained intracellularly for presentation of the antigen days later when monocyte-derived DCs migrated to lymph nodes or in vitro after differentiation with granulocyte/macrophage colony-stimulating factor. These data reveal that immature monocytes unexpectedly sample antigen from the bone marrow environment and that they can present these antigens after they leave the bone marrow.

CORRESPONDENCE
Gwendalyn J. Randolph:
Gwendalyn.Randolph@mssm.edu

Abbreviations used: CLL, clodronate-loaded liposome; FSC, forward scatter; LX, latex; PT, pertussis toxin.

Monocytes are established precursors for macrophages and DCs. Once monocytes emigrate across the endothelial lining of the bloodstream, they rapidly begin the process of differentiation to one or the other of these terminal phenotypes (1–3). Thus, as the life cycle of the monocyte is mainly confined to the blood and bone marrow, it would seem unlikely that monocytes directly participate in activities like the clearance of apoptotic cells or the presentation of antigen to T cells other than by serving as precursors for the DCs and macrophages that perform these tasks. However, it is recognized that different subpopulations of monocytes may differ in their capacity to develop particular phenotypes or specializations once recruited to a given tissue (4–9).

Macrophages play a major role in clearing dead or dying cells (10, 11). DCs also engulf apoptotic cells and can cross-present antigens from these cells to elicit T cell responses (11). Freshly isolated monocytes lack the capacity to take up apoptotic cells in vitro (12–14), but they may rapidly differentiate and acquire the ability to take up apoptotic cells at sites of acute inflammation, where they appear to be critical in removing the mass of dying neutrophils (15). Besides sites of acute inflammation, the bone marrow is another place where many cells continually undergo apoptosis. There, for example, macrophages are involved in clearing the large number of B lineage cells that fail to successfully recombine genes encoding Ig (16). Furthermore, senescent neutrophils efficiently home to the bone marrow (17), presumably for clearance by bone marrow macrophages.

The fate of apoptotic cells after engulfment by macrophages versus DCs is expected to be decidedly different. DCs initiate immune responses and cannot be replaced by macrophages for immune priming even for immune presentation of microbes like *Listeria monocytogenes* that efficiently infect macrophages (18). An important factor that enables DCs to present epitopes from phagocytized material, apparently including apoptotic cells (19, 20), is the poor proteolytic activity they possess in the endosomal/lysosomal compartments (21),

The online version of this article contains supplemental material.

as this property permits the retention of peptides for presentation to T cells. Indeed, DCs can intracellularly retain peptides/antigen for at least 2 d (22), seemingly in waiting for conditions that induce their maturation and consequently promote the display of the retained peptides on surface MHC molecules. Macrophages, on the other hand, robustly degrade the phagocytic antigens that they engulf (21) such that these antigens are readily destroyed and, therefore, may fail to promote T cell priming. The expression of cathepsins, the main enzymes responsible for the degradation of proteins within intracellular compartments, by blood monocytes mirrors their pattern of expression in macrophages qualitatively and quantitatively (23). However, in monocytes, cathepsin activity is mostly found in endosomes and later becomes shifted to lysosomes during maturation to macrophages (23). This difference may impact how efficiently monocytes degrade ingested material because endosomally localized proteolysis may spare peptides for antigen presentation over the more robust proteolysis in lysosomes (24).

In this study, we initially set out to develop techniques to trace monocyte subsets in vivo that did not rely on adoptive transfer. We could stably label Gr-1^{lo} monocytes with a particulate latex (LX) bead by injection of the beads i.v. However, the labeling of Gr-1^{hi} monocytes required that we introduce LX beads i.v. in the absence of circulating monocytes. In this case, bone marrow monocytes acquired the phagocytic label and emerged from the bone marrow as the more immature Gr-1^{hi} monocyte subset. Acquisition of the label by bone marrow Gr-1^{hi} monocytes resulted from prior labeling of other cells, particularly marginal zone B cells and neutrophils, that first carried the particles to the bone marrow and transferred them to bone marrow monocytes. Ultimately, we show that B cell antigens themselves are acquired by bone marrow monocytes, implying that monocytes engulf whole cells during the transfer of antigens and that the acquisition of this antigen permits presentation of the epitopes much later, after monocytes have entered the periphery and further differentiated. These observations unexpectedly reveal that monocytes can phagocytize material, including other cells, in the bone marrow before entering the circulation. This activity can lead to the induction of immune responses to the engulfed antigens later in the periphery. We discuss how these findings may also bear on the capacity of monocytes to act as Trojan horses for the spread of microorganisms like *Listeria monocytogenes*.

RESULTS

Labeling of blood monocyte subsets with phagocytic tracers

Labeling of Gr-1^{lo} monocytes. Fluorescent LX microspheres can be used to selectively track the migration of monocyte-derived DCs from skin to the draining lymph node (7, 25). Therefore, we tested whether the systemic application of microspheres via i.v. injection would similarly selectively label monocytes in the circulation. Blood monocytes coexpress CD115 (macrophage CSF receptor) and F4/80 (Fig. 1 A; references 7, 26), and they are divisible as three different subpopulations according to whether they express high, intermediate, or low levels of Gr-1 (Ly6C/G; Fig. 1 A; references 6, 7, 26). Within 4 h after i.v. injection of LX particles, 1–2% of all cells in the circulation become LX$^+$ (Fig. 1 B). Most LX$^+$ cells were monocytes; they accounted for two thirds of LX$^+$ cells at 4 h (Fig. 1 B) after injection and ~90% thereafter. Overall, ~10–12% of blood monocytes were phagocytically labeled using this approach (Fig. 1 B).

In the first 2 h after LX bead injection, the relative frequency of LX bead uptake among monocyte subsets mirrored the overall frequency of the subsets in the whole monocyte population, with nearly half of the LX$^+$ cells expressing high levels of Gr-1 (Fig. 1 C). However, within 4 h after injection, these LX$^+$ Gr-1^{hi} monocytes had converted to the Gr-1^{int} and Gr-1^{lo} subsets, subsequently resulting in only Gr-1^{lo} LX$^+$ monocytes by 24 h (Fig. 1 C). Meanwhile, the frequency of the various subsets in the whole monocyte fraction remained unaltered (Fig. 1 C). Gr-1^{lo} LX$^+$ monocytes persisted in the circulation for >1 wk, but the percentage of LX$^+$ monocytes decreased gradually from nearly 10% at day 1 to ~5% by day 7 (Fig. 1 D).

Besides the particle-labeled CD115$^+$F4/80$^+$ monocytes in the circulation, we observed a large reservoir of LX$^+$ cells in the splenic marginal zone (Fig. 1 E, micrograph). Some of these cells were CD11b^{hi} macrophages (Fig. 1 E, left flow plot), but the majority unexpectedly were marginal zone B220$^+$CD19$^+$ B cells (Fig. 1 E, right flow plot). In contrast to abundant LX$^+$ B cells in the marginal zone, very few LX$^+$ cells were present within B cell follicles (Fig. 1 E, micrograph). Although marginal zone B cells in the spleen acquired microspheres, they remained resident therein and were not or were only scarcely detected in other examined tissue (blood, bone marrow, peripheral lymph nodes, and skin) for at least 7 d (not depicted). Thus, i.v. injection of LX microspheres stably labels circulating Gr-1^{lo} monocytes, whereas some Gr-1^{hi} monocytes were transiently labeled and rapidly converted to Gr-1^{lo} monocytes.

Labeling of Gr-1^{hi} monocytes. As previously published, monocytes can be rapidly and efficiently (>95%) eliminated from the circulation by the systemic administration of clodronate-loaded liposomes (CLLs; references 7, 26, 27). Injection of CLLs i.v. results in the depletion of blood monocytes by 18 h (26) accompanied by the full depletion of macrophages from the spleen and a transient reduction, but not full depletion, of CD115$^+$ monocytes from the bone marrow (Fig. 2, A and B; and not depicted). Marginal zone DCs are completely abolished by CLL (28), but white pulp DCs are not affected, which is consistent with our observation that splenic CD11c$^+$ cells were reduced by up to 50%. As previously shown (26), monocytes began to reappear in blood ~40 h after CLL injection (Fig. 2 A).

Injection of LX particles i.v. 18 h after CLL administration (Fig. 2 C), when monocytes were absent from the blood, unexpectedly did not prevent the labeling of blood monocytes

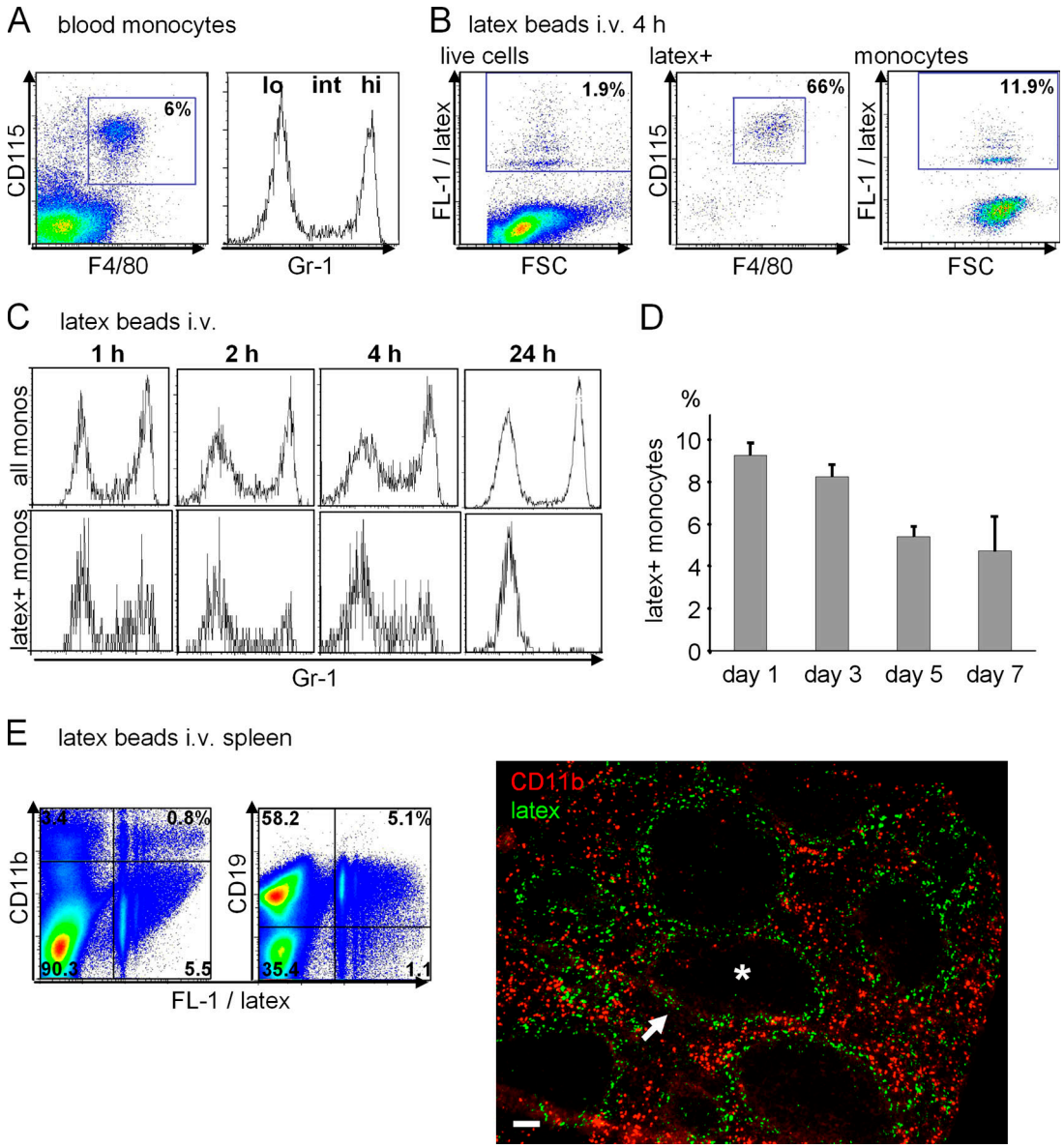

Figure 1. Labeling of Gr-1^{lo} monocytes by i.v. LX particles. (A) Monocytes were identified as low SSC CD115$^+$ F4/80$^+$ live cells, and subsets were defined by surface Gr-1 levels (lo, low; int, intermediate; hi, high). (B) Blood analysis 4 h after i.v. LX bead injection. Gates on total live cells, LX$^+$ cells, or monocytes are shown. Data are representative of >20 experiments. (C) Short-term time course of the Gr-1 phenotype of LX$^+$ monocytes (monos) or all monocytes after i.v. administration of LX beads in the blood ($n = 6$ at each time point). (D) LX labeling efficiency of Gr-1^{lo} monocytes expressed as the percentage of all monocytes. Data are the means ± SEM (error bars) of >10 animals per time point. (E) Analysis of spleen after i.v. injection of LX particles. FACS analysis 4 h after LX injection identifies most LX$^+$ cells in the spleen as B220$^+$CD19$^+$ B cells and fewer CD11b^{hi} macrophages. (right) Sections of spleen 1 d after i.v. LX administration stained for CD11b (red) show LX beads (green) in the marginal zone (arrow) but not in white pulp (asterisk). Bar, 100 μm.

with the microspheres. Instead, LX$^+$ monocytes still appeared in the blood when circulating monocytes were reestablished after their CLL-mediated transient depletion (Fig. 2 C). Labeling efficiency was 10–15% of the total blood monocyte pool (Fig. 2 C). In contrast to the fate of the monocytes that took up beads without prior monocyte depletion (Fig. 1), LX$^+$ blood monocytes that reappeared after transient monocyte depletion did not rapidly convert to Gr-1^{lo} monocytes; instead, they remained Gr-1^{hi} for ∼7 d, when they then began to convert into Gr-1^{int} and Gr-1^{lo} subsets (Fig. 2 C). Their frequency in blood was only slightly reduced over a 7-d period (Fig. 2 C, bar graph). Thus, this method that involves an initial monocyte depletion step leads to stable labeling of Gr-1^{hi} blood monocytes, which is in contrast to the aforementioned protocol that leads to the labeling of Gr-1^{lo} monocytes (Fig. 1).

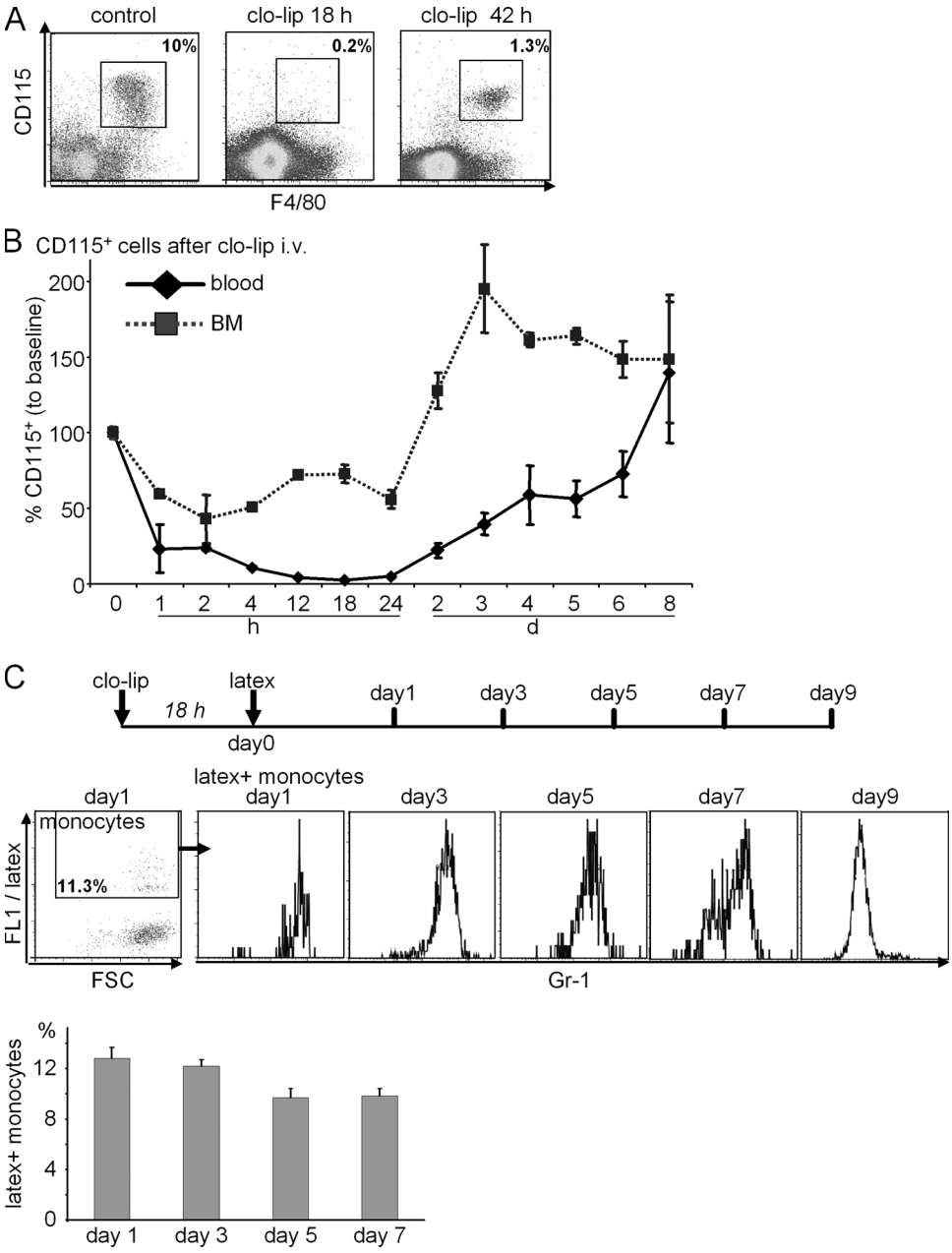

Figure 2. Labeling of Gr-1^{hi} monocytes by i.v. clodronate liposomes followed by LX particle injection. (A) Flow cytometric evaluation of blood monocytes. By 18 h after i.v. injection of CLLs (clo-lip), >95% of all blood monocytes are depleted from the circulation. 1 d later (42 h after clo-lip), monocytes reappear in the blood (right plot). (B) Flow cytometric evaluation monitored the presence of monocytes in blood and bone marrow at various time points after CLLs were injected i.v. The line graph illustrates the degree of depletion in blood and bone marrow through 8 d. Results are expressed as the percent frequency of monocytes ± SEM (error bars) compared with their starting baselines in blood and bone marrow (BM). (C) Injection schedule for the labeling of Gr-1^{hi} monocytes in circulation is depicted. The labeling of returning blood monocytes with LX at day 1 is shown (dot plot). Histograms reveal the intensity of Gr-1 on the LX$^+$ returning monocytes, and the bar graph indicates the LX labeling efficiency of Gr-1^{hi} blood monocytes (mean ± SEM). More than eight animals were examined and showed similar results per time point; individual animals are shown.

LX particle transfer to bone marrow monocytes from B cells and neutrophils

We next wondered how monocytes became labeled with particles after CLL depletion because monocytes were not present in the circulation when LX beads were injected therein. Few free particles were observed in blood at the time when monocytes began to return after depletion (Fig. S1, available at http://www.jem.org/cgi/content/full/jem.20052119/DC1), so it seemed unlikely that the nascent monocytes would encounter free particles during their labeling. Indeed, our investigation

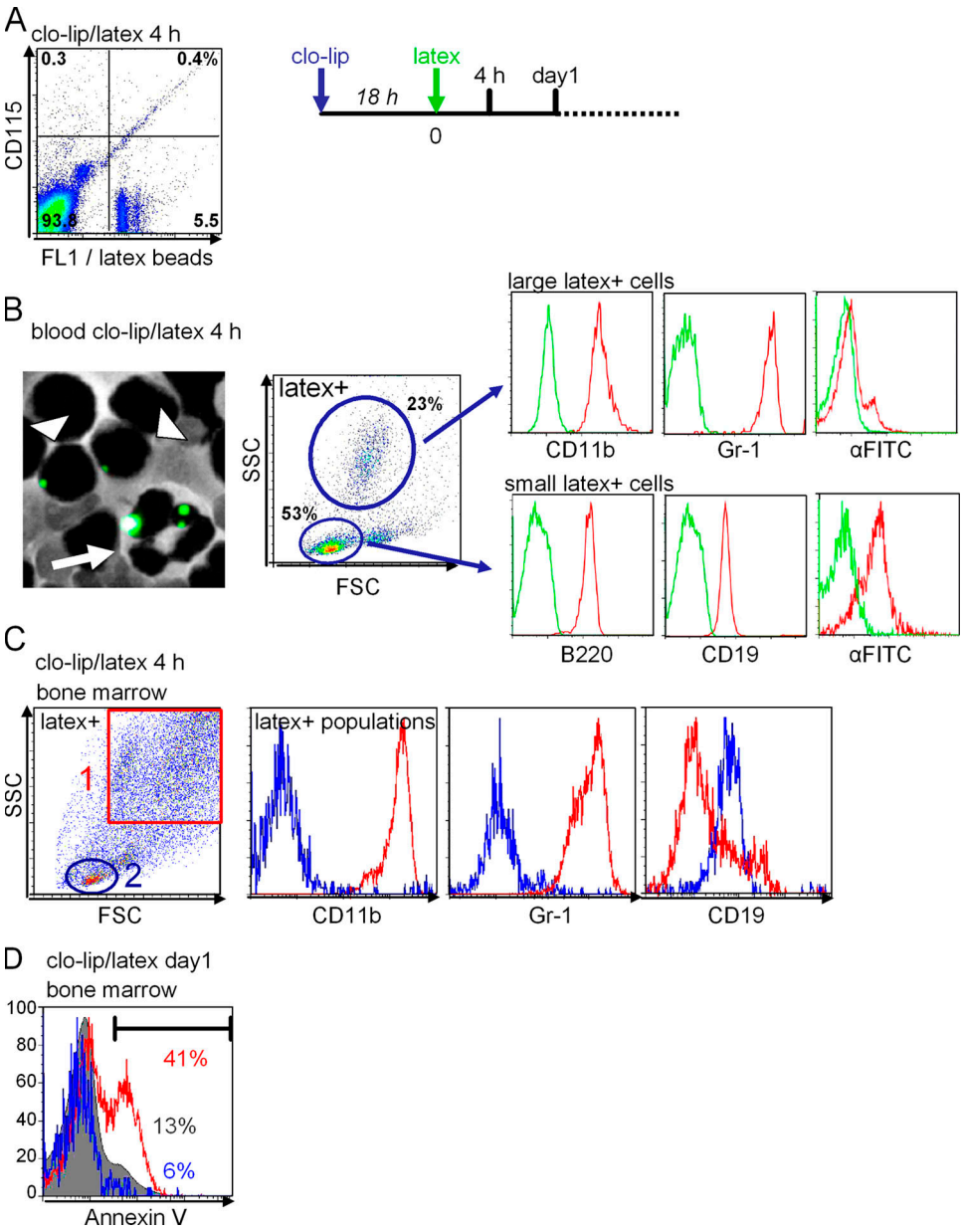

Figure 3. Labeling of blood B cells and neutrophils during monocyte depletion. (A) The injection scheme, as depicted, was to administer CLLs and, 18 h later, when monocytes were depleted, to inject LX beads i.v. The blood was examined for LX^+ cells 4 h thereafter. LX^+ cells at this time point were $CD115^-$ cells. (B) The LX^+ $CD115^-$ blood cells during monocyte depletion (4 h after LX administration; see injection scheme in A) was comprised of two populations: small lymphocytes (arrowheads in cytospin) that stain positive for B220, CD19, and anti-FITC and large neutrophils (arrow in cytospin) that stain positive for CD11b and Gr-1 and negative for anti-FITC. Red lines in each profile reveal staining for these molecules; green lines reveal staining with isotype-matched control mAbs. Data are representative of at least six mice analyzed individually per condition. (C) The bone marrow in mice subjected to the injection scheme in A and examined 4 h after LX was administered i.v. shows populations with similar profiles as in the blood. Gates of LX^+ cells in bone marrow reveal small cells with low SSC (gated blue in the FSC/SSC plot) and larger cells with high side scatter (gated red in the FSC/SSC plot). Histograms show staining patterns of these populations in the same color as the corresponding gate. (D) The occurrence of apoptotic cells in the bone marrow was monitored by annexin V staining in mice injected with CLLs followed by LX particles (as per the injection scheme in A). The bone marrow was examined 1 d after LX beads were administered i.v. The gray histogram represents gates on all cells, the blue line represents gating on small LX^+ cells (B cells; blue gate in C), and the red line represents gating on large LX^+ cells (neutrophils; red gate in C). Percentage of annexin V–positive cells (bar) is shown.

into this question, detailed in this section, illustrated that the particles were transferred via other cell types that first acquired them in the absence of monocytes.

Fig. 2 delineated our detection of LX^+ monocytes at the time points (day 1 and beyond) when monocytes returned to blood after depletion. When we examined blood after LX

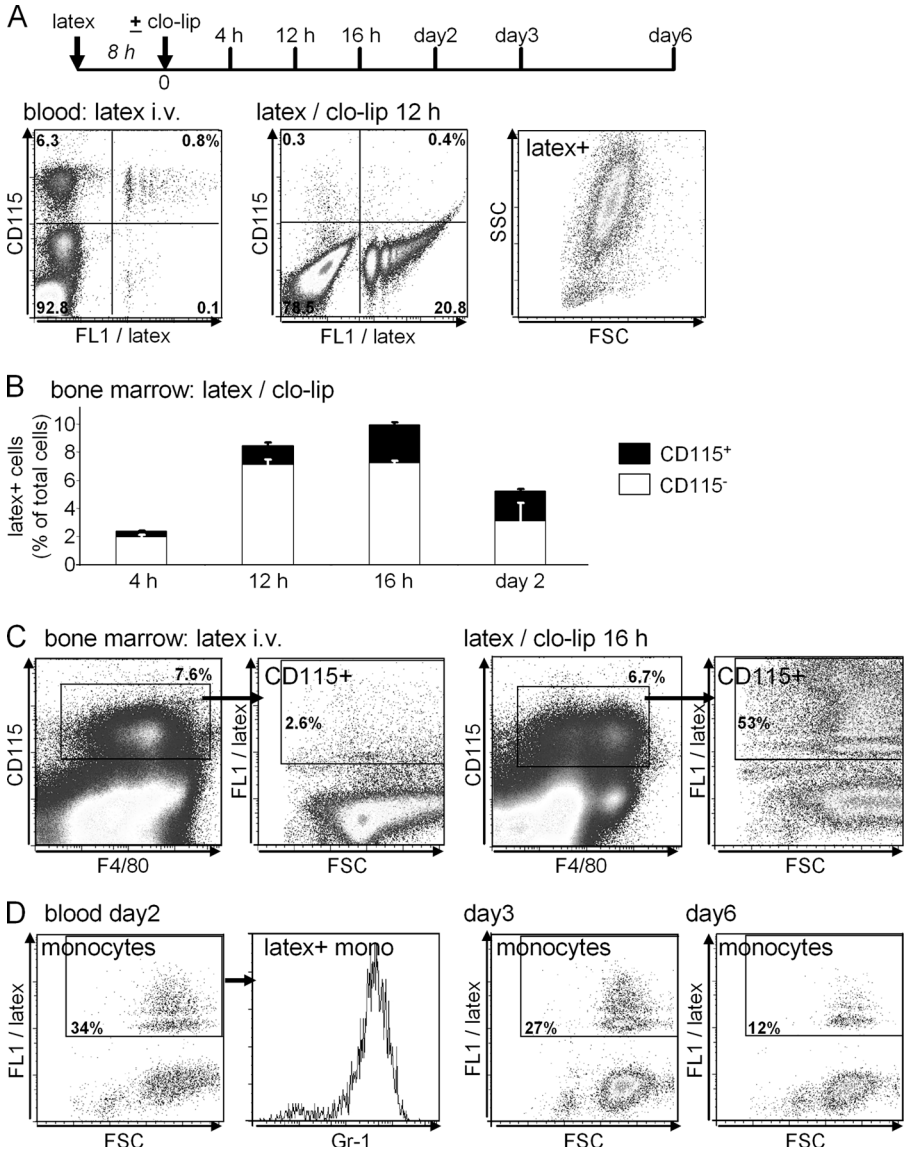

Figure 4. Mobilization of LX$^+$ neutrophils and B cells from the spleen to the bone marrow leads to robust monocyte labeling. (A) LX beads were injected i.v. Then, 8 h later, some mice received CLLs i.v. (middle dot plot). The blood was analyzed 12 h later, 20 h after the administration of LX beads, and at several time points thereafter. At the 12-h time point, most LX$^+$ cells seen in the group of mice receiving CLLs were CD115$^-$ cells with the high FSC/SSC profile of neutrophils (middle and right dot plots). A comparison with mice receiving no liposomes, only LX i.v., is shown in the left dot plot. (B) A time course depicts the fraction of LX$^+$ cells among total bone marrow cells that were CD115$^-$ (mostly neutrophils and B cells) and CD115$^+$Gr-1^{hi} monocytes from 4 h to 2 d after the administration of CLL. Error bars represent SEM. (C) Bone marrow was analyzed 16 h after liposome administration. Monocytes were identified by double staining for F4/80 and CD115, and the degree to which this population was LX$^+$ was assessed (right plots). Comparison was made with mice that received only LX beads without CLL (left plots). (D) Analysis of the monocyte population in blood at day 2 or later after CLLs were administered. All data are representative of more than six mice per condition.

particle administration but before CD115$^+$ monocytes reappeared, we observed the presence of LX particles in CD115$^-$ blood cells (Fig. 3 A). When we sampled blood 4 h after the i.v. administration of LX beads, 20–25% of LX$^+$ cells in the circulation were neutrophils, as indicated by their high forward scatter (FSC)/SSC profile (Fig. 3 B, dot plot), typical nuclear morphology (Fig. 3 B, arrow in photomicrograph), positive reactivity with mAbs to CD11b, Gr-1, and CD62L, and negative reactivity with mAbs to CD115, CD3, CD4, CD8, B220, CD19, I-A^b (MHC-II), DX5, and NK1.1 (Fig. 3 B, histograms; and not depicted). The LX particles associated with these neutrophils had been phagocytically internalized, as they were inaccessible to reactivity with anti-FITC mAb (Fig. 3 B, histogram).

In addition to labeled neutrophils, between 50–60% of the blood LX$^+$ cells found in the absence of monocytes were

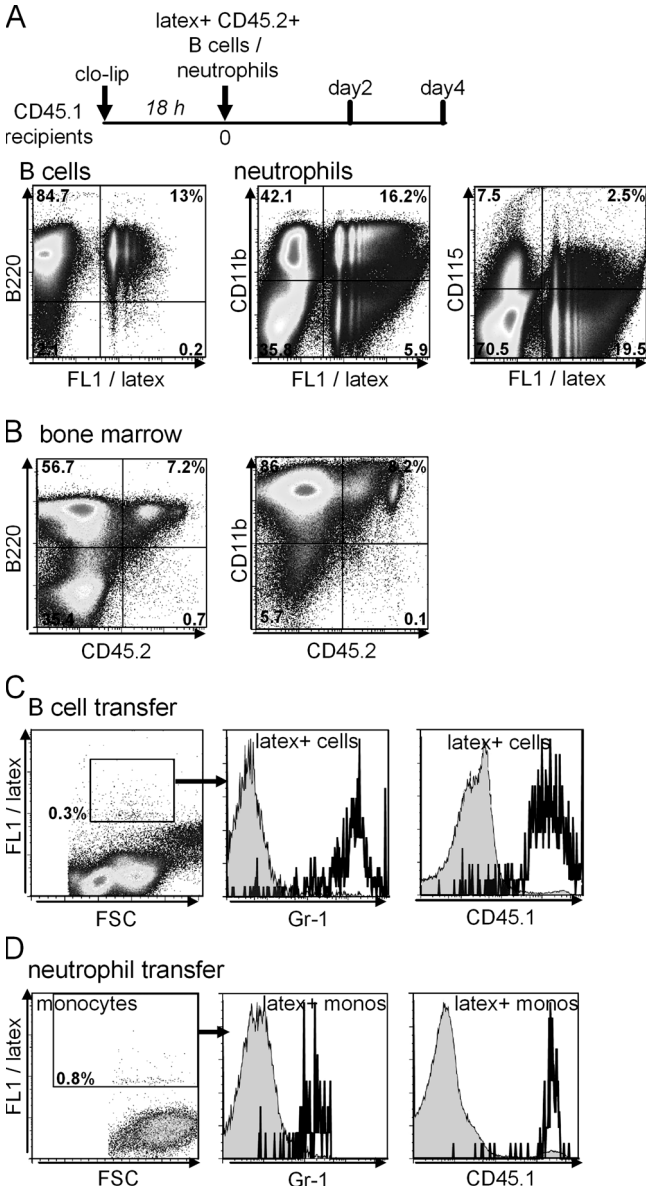

Figure 5. Adoptive transfer of LX$^+$ CD45.2$^+$ B cells and neutrophils into CD45.1$^+$ recipient mice. (A) For the isolation of B cells for adoptive transfer, donor mice were treated first with CLL and then with LX beads i.v as described in Materials and methods. B220$^+$ cells were positively selected using magnetic cell sorting beads, and 15–20% of these B cells were LX$^+$. Cells enriched with LX$^+$ neutrophils (CD11b$^+$ CD115$^-$ cells with high SSC) were prepared by incubating total bone marrow cells ex vivo with LX beads. A minor population (<3% of total cells) of this cell preparation were LX$^+$ monocytes, shown by CD115 staining (right plot). (B) Bone marrow was analyzed 2 d after adoptive transfer, when blood monocytes were beginning to return. CD45.2$^+$ transferred cells were present when either labeled B cells (left) or neutrophils (right) were transferred. (C and D) In the circulation of recipient mice that received adoptively transferred LX$^+$ B cells (C) or cell preparations enriched in neutrophils (D) 18 h after the administration of CLL, CD115$^+$ monocytes were observed that became LX$^+$ (left), were Gr-1hi (black lines, middle; gray line identifies Gr-1lo control staining), and were CD45.1$^+$ (right, black lines; gray lines represent negative control staining). The intensity of Gr-1 staining on Gr-1^{hi} cells varies from C because of the use of a different anti–Gr-1 conjugate. In each experimental design, at least six mice were recipients of adoptively transferred cells (three experiments conducted in duplicate), and each showed similar outcomes.

B cells, as determined by their low FSC/SSC profile (Fig. 3 B, dot plot), typical lymphocytic morphology (Fig. 3 B, arrowheads in photomicrograph), positive reactivity with mAbs to B220, CD19, I-A^b, and CD62L, and negative reactivity with mAbs to CD115, F4/80, Gr-1, CD11b, CD3, CD4, CD8, DX5, and NK1.1 (Fig. 3 B, histograms; and not depicted). In contrast to the neutrophils, the LX particles associated with B cells were present on the cell surface and were not internalized because most of these cells reacted positively with anti-FITC mAb (Fig. 3 B).

Recalling that even in the continuous presence of monocytes, a major reservoir of LX$^+$ CD19$^+$B220$^+$ marginal zone B cells after the injection of particles was sequestered in the spleen (Fig. 1), it seemed likely that the depletion of marginal zone splenic macrophages by CLLs initiated mobilization of marginal zone B cells to the blood. Marginal zone macrophages normally interact with marginal zone B cells (29), so it is reasonable that when LX beads are administered in the absence of monocytes and marginal zone macrophages, some LX$^+$ marginal zone B cells become diverted to the circulation. Besides being present in blood, the two populations of CD115$^-$ LX$^+$ cells also homed to bone marrow (Fig. 3 C). LX$^+$ neutrophils were identified by their FSC/SSC profile and because of their high Gr-1 and CD11b expression (Fig. 3 C); B cells were CD19$^+$B220$^+$ (Fig. 3 C). The presence of a few CD19+ cells in the high SSC gate (gate 1; Fig. 3 C) suggests that some B cells may associate with neutrophils. LX$^+$ B cells mainly bearing only a single bead per cell dispersed systemically. Besides trafficking to bone marrow, they additionally homed to lymph nodes (unpublished data). Neutrophils arriving in the bone marrow were clearly undergoing apoptosis, as a substantial fraction of them stained positively with annexin V within the first day after their arrival (Fig. 3 D). We observed only a few annexin V$^+$ LX$^+$ B cells, so it remains unclear how many of the B cells were undergoing apoptosis shortly after arrival in the bone marrow. Nonetheless, the appearance of LX$^+$ B cells in the bone marrow, like neutrophils, was transient. By day 2 after the appearance of these populations in the bone marrow, the frequency of these cells was reduced in the bone marrow, as the appearance of LX$^+$ monocytes began instead to emerge in blood and bone marrow (Figs. 2 and 4). Therefore, the survival of LX$^+$ neutrophils and B cells in the bone marrow is likely relatively brief.

To further test whether it was the dispersion of numerous LX$^+$ neutrophils and B cells to the blood or bone marrow that led to the delivery of particles to the Gr-1^{hi} monocyte population, we inversed the order of monocyte depletion and particle labeling such that particle-bearing cells were first sequestered in the spleen before potentially becoming mobilized by the introduction of CLLs. Thus, LX

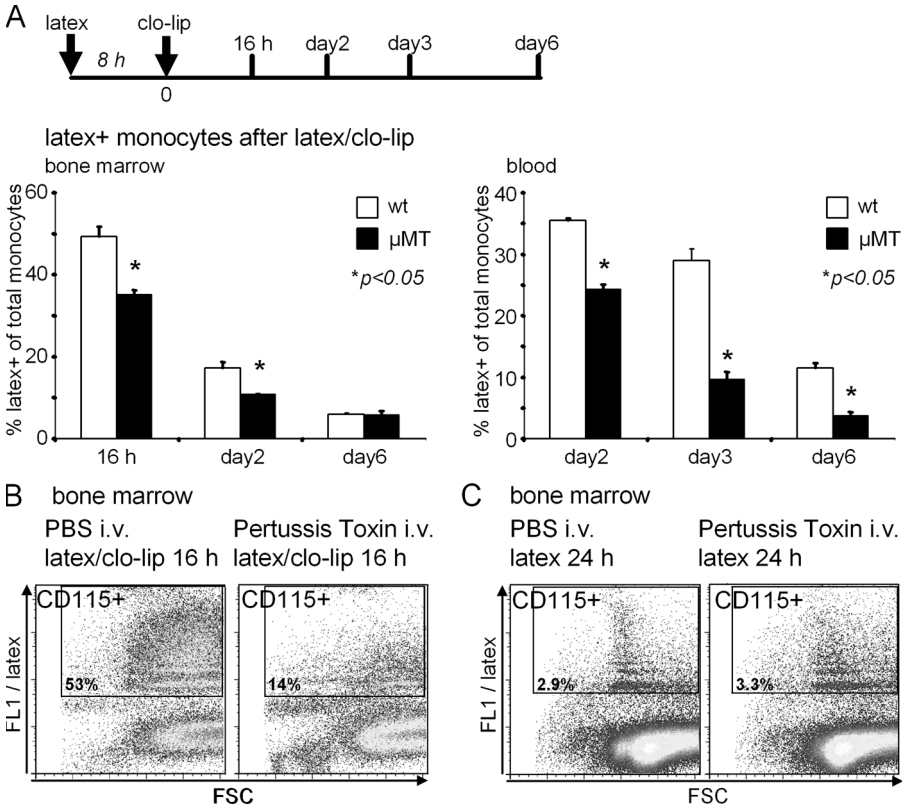

Figure 6. Effect of B cell deficiency and PT on the transfer of LX to bone marrow monocytes. (A) C57BL/6 WT (white bars) and B cell–deficient μMT mice (black bars) were treated i.v. with LX particles followed by CLLs as diagramed in the schematic. The percentage of $CD115^+$ monocytes that were LX^+ in bone marrow and blood is depicted. Results are expressed as means ± SEM (error bars); differences between WT and μMT mice at most time points are significant (*, $P < 0.05$ using a *t* test). (B) LX beads were administered to mice, and mice received CLL i.v. 8 h later along with PT or PBS. Bone marrow was examined at 16 h to assess the impact of PT treatment on the acquisition of LX by monocytes. Data are representative of three mice in each condition, all with similar outcomes. (C) Mice received PT or PBS i.v. followed by LX beads i.v. 2 h later, and bone marrow was examined after 24 h for LX particle uptake by monocytes. Data shown are representative of three mice in each condition, all with similar outcomes.

particles were injected i.v. first, and CLLs were injected 8 h later (Fig. 4 A, schematic depiction of injection scheme). The number of LX^+ cells in the circulation was dramatically increased by this approach compared with the injection of LX alone (Fig. 4 A), such that 20% of the leukocytes in blood were LX^+ 12 h after CLL injection compared with only 0.8% (~10% of monocytes) of leukocytes in the blood of mice that received LX beads i.v. but not CLLs (Fig. 4 A). In this protocol, as in Fig. 3, the LX^+ cells were again $B220^+CD115^-$ B cells and $CD11b^+Gr\text{-}1^+CD115^-$ neutrophils, but the majority by this protocol were neutrophils (FSC/SSC profile; Fig. 4 A and not depicted). In bone marrow, by 4 h after the dispersion of LX^+ cells from the spleen using CLL, >2% of the bone marrow was LX^+, and nearly all of these cells were $CD115^-$ B cells and neutrophils (Fig. 4 B and not depicted). By 12 h, LX^+ cells continued to increase in the bone marrow, and a greater fraction was $CD115^+$. $CD115^+$ cells accounted for an increasingly greater proportion of the LX^+ cells in the bone marrow at 16 h and day 2, as the frequency of LX^+ $CD115^-$ cells declined by day 2, and the LX^+ $CD115^+$ cells in the bone marrow reached an equilibrium (Fig. 4 B).

At 16 h after CLL injection, ~50% of the bone marrow $CD115^+$ cells were LX^+ (Fig. 4 C). In contrast, only ~3% of the $CD115^+$ bone marrow cells were LX^+ at this same time point when LX beads were administered i.v. in the absence of blood monocyte depletion (CLL treatment). During the first 24 h after CLL administration, there were no circulating monocytes as a result of the depletion mediated by CLLs. However, at day 2 (40 h after CLL injection), 35% of the returning monocytes in blood were LX^+ and $Gr\text{-}1^{hi}$ (Fig. 4 D), mirroring the high labeling of bone marrow precursors at day 1. The fraction of LX-labeled monocytes remained high for at least several days, with 25% of blood monocytes being LX^+ at day 3 and 12% at day 6 (Fig. 4 D).

These experiments were consistent with the possibility that monocyte precursors in the bone marrow may have engulfed particle-bearing B cells and neutrophils that homed to the bone marrow after release from the spleen, leading to their own labeling with LX before entering the circulation

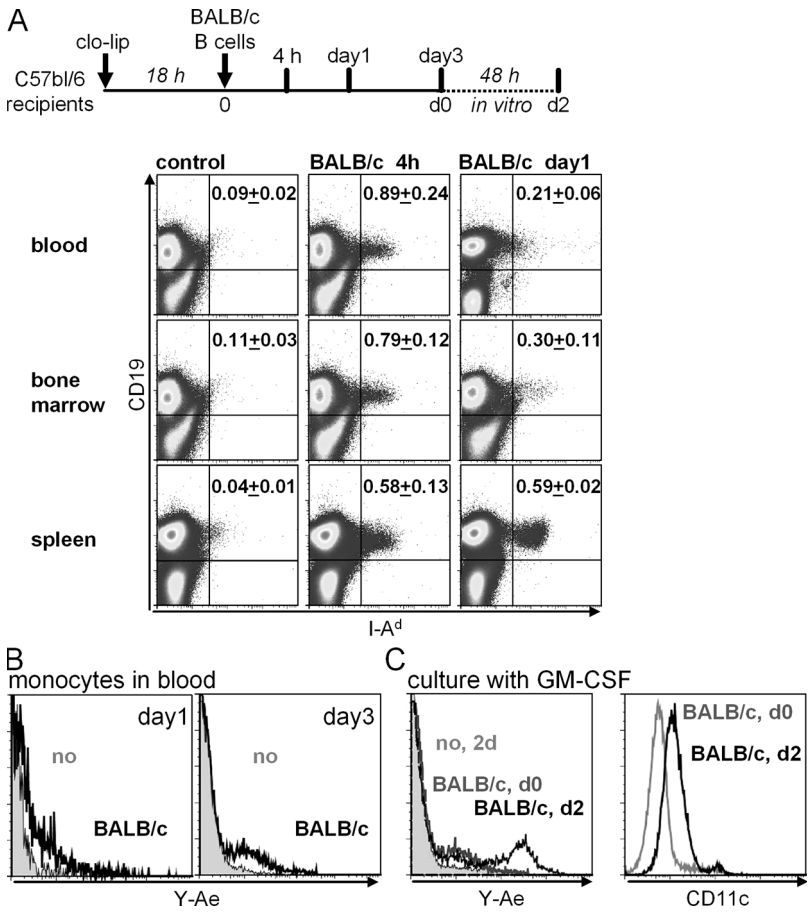

Figure 7. Antigen presentation of cellular proteins from transferred allogeneic B cells to monocytes. (A) I-A^{d+} B cells were isolated from spleen and lymph nodes of BALB/c mice and injected i.v. into monocyte-depleted C57BL/6 mice 18 h after treatment with CLLs as shown in the schematic. Monocyte-depleted mice that did not receive BALB/c B cells served as controls. The presence of I-A^{d+} B cells was analyzed in blood, bone marrow, and spleen 4 h and 1 d after B cell transfer. Cells with a low FSC/SSC profile were gated to focus analysis on lymphocytes, and the percentage of $CD19^+IA^{d+}$ lymphocytes was determined. Each plot shows the mean + SD of at least three mice studied per condition. (B) Histograms show Y-Ae expression on blood monocytes at days 1 and 3 (gray histogram, controls; black line, BALB/c B cell transfer). Six animals per condition were studied in three independent experiments. (C) Whole blood cells were prepared 3 d after BALB/c cell transfer i.v., and washed leukocytes were cultured for 2 d in the presence of GM-CSF to promote the differentiation of monocytes toward a DC phenotype. Y-Ae (left) and CD11c (right) expression by monocytes was examined after BALB/c B cell transfer before (dark gray line) and after (black line) culture; gray histogram, control monocytes from mice not receiving transferred B cells after 2 d of culture (no).

as Gr-1^{hi} monocytes. To further explore whether B cells and neutrophils that acquire LX microspheres during monocyte depletion might transfer particles to immature monocytes in the circulation or possibly to bone marrow monocyte precursors, we adoptively transferred LX^+ $B220^+$ B cells (Fig. 5 A) and/or cell preparations enriched with $CD11b^+CD115^-$ LX^+ neutrophils (Fig. 5 A) from $CD45.2^+$ (Ly5.2) donors into $CD45.1^+$ (Ly5.1) transgenic mice that had earlier received CLLs. $CD45.2^+$ LX^+ B cells and neutrophils were observed to home to the bone marrow (Fig. 5 B); the fractions of $CD45.2^+$ cells recovered in the bone marrow that were also LX^+ were 15 and 5%, respectively. After the transfer of either cell type and recovery of blood monocyte pools, LX^+ Gr-1^{hi} $CD45.1^+CD45.2^-$ monocytes appeared in the circulation (Fig. 5, C and D), although the efficiency of monocyte labeling with adoptively transferred cells (<1% of all monocytes) was reduced compared with the labeling that occurs endogenously (Figs. 2–4). These data indicate that monocyte labeling with LX indeed occurs through the transfer of LX beads by other cells, in this case by neutrophils or B cells.

Kinetic studies revealed that bone marrow monocytes were substantially LX^+ by 16 h after CLLs were administered to mice that were previously treated to label LX^+ B cells and other cells in the spleen (Fig. 6 A, injection schematic). At 16 h, mobilized LX^+ B cells and neutrophils have already reached the bone marrow at least several hours earlier (Fig. 4 B) and are undergoing transfer to bone marrow monocytes by this time (Figs. 4 B and 6 A, left bar graph). In mice lacking B cells (μMT mice), the labeling efficiency of bone

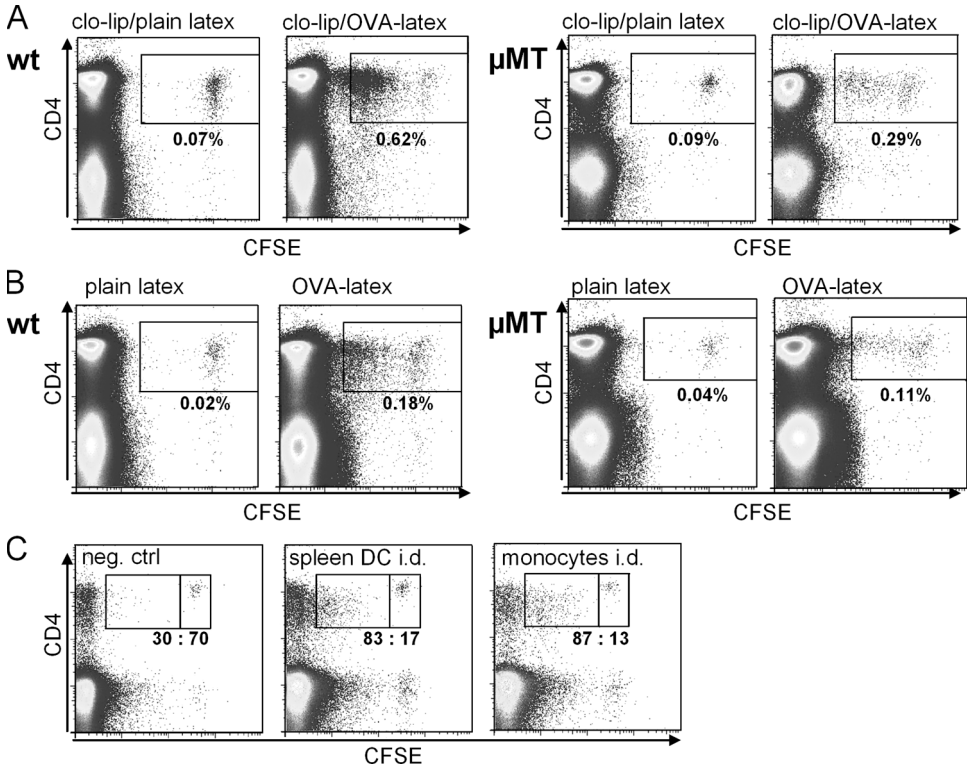

Figure 8. Antigen presentation by Gr-1^{hi}– and Gr-1^{lo}–labeled monocytes and induction of T cell proliferation in vivo. (A) CD4$^+$ OT-II cells pooled from spleen and lymph nodes by positive selection for CD4 expression were labeled with CFSE and injected into CLL-treated C57BL/6 wt mice (left) or B cell–deficient µMT mice (right) that had also received either plain (not conjugated) LX beads or OVA-conjugated LX beads. (B) A similar experimental design was performed except that mice were not treated with CLL, such that Gr-1^{lo} monocytes became LX$^+$. (A and B) These data are representative of three experiments with two mice per group. (C) OVA-LX–labeled monocytes (splenic DCs were positive controls) were isolated from bone marrow and injected intradermally into the back skin and front footpad of MHC-II$^{-/-}$ mice, which had received CFSE-labeled OT-II cells. Proliferation of CFSE-labeled OT-II cells was assessed at day 6. A gate was drawn around CFSE-labeled T cells in each mouse. The number accompanying the left side of the box indicates percent proliferated CFSE-labeled T cells; the number marking the right side of the box indicates the fraction of CFSE-labeled T cells that did not proliferate.

marrow monocytes was somewhat reduced, which is consistent with the possibility that B cell migration to bone marrow is necessary for optimal monocyte labeling (Fig. 6 A). This reduced labeling of bone marrow monocytes in µMT mice was accompanied by a subsequent reduction of blood monocyte labeling after monocytes reappeared in the circulation at day 2 (Fig. 6 A). Therefore, we next examined the effect of blocking the trafficking of both neutrophils and B cells to the bone marrow. Both B cells and neutrophils at least partly use the G_i protein–coupled chemokine receptor CXCR4 to home to the bone marrow (17, 30). Thus, we determined whether pertussis toxin (PT) would impair the postulated cell-mediated transfer of particles to bone marrow monocytes. PT-treated mice showed blood neutrophilia and increased numbers of neutrophils in the spleen but reduced bone marrow neutrophils (unpublished data). When PT was injected i.v. during the periods when CLLs and LX were administered, the labeling of bone marrow monocytes with LX was dramatically reduced compared with PBS-injected controls (Fig. 6 B). Instead, LX$^+$ neutrophils were abundantly found in the blood and spleen (not depicted). The relatively smaller number of bone marrow monocytes that acquires LX in the bone marrow when CLL is not used to mobilize neutrophils and B cells from spleen (Fig. 4 C, LX i.v.) was unaffected by the prior administration of PT (Fig. 6 C), indicating that PT did not directly affect the phagocytic activity of bone marrow monocytes. Therefore, the reduced labeling of bone marrow monocytes in the presence of PT after CLL treatment supports the conclusion that the degree of homing of LX$^+$ neutrophils and B cells to the bone marrow directly affects how efficiently Gr-1^{hi} monocytes become labeled with LX. These data collectively show that B cells or neutrophils pass particulate antigens to monocytes and illustrate that the bone marrow is the major site of particulate antigen transfer.

Processing and presentation of transferred antigens

Because neutrophils phagocytized LX particles and carried them intracellularly, the transfer of neutrophil-associated particles to monocytes suggests that the monocytes engulfed the neutrophil after its arrival into the bone marrow. However, because B cells carried the particles on their surface, it

was not clear whether the transfer of particles to monocytes from B cells involved the engulfment of dying B cells. To assess this possibility definitively and to determine whether any processed cell antigen was routed by the monocyte for display to T cells, we determined whether the adoptive transfer of BALB/c B cells into C57BL/6 hosts would lead to reactivity of the monocytes with the Y-Ae antibody. This mAb reacts with a peptide derived from I-Eα of BALB/c donor cells presented in the context of I-A^b (19, 31).

BALB/c B cells were prepared by minimagnetic cell sorting separation, and 5 million were transferred to CLL-treated C57BL/6 recipients i.v. Although it would be expected that the majority of these B cells would die spontaneously or in response to NK cell–mediated killing after transfer, we observed that the trafficking of allogeneic B cells was strikingly similar to the mobilization of LX^+ B cells to the bone marrow (Fig. 3). 4 h after transfer, BALB/c B cells, identified as $CD19^+$ IA^{d+} cells, were found in the blood, bone marrow, and spleen (Fig. 7 A). By 24 h, transferred cells were scarcely detectable in the blood, were greatly reduced in the bone marrow, but remained detectable in the spleen (Fig. 7 A).

1 and 3 d later, we analyzed whether any of the monocytes expressed the Y-Ae epitope, which is indicative of processing and presenting BALB/c B cells. To control for the specificity of the Y-Ae mAb, we stained monocytes from C57BL/6 mice that did not receive adoptively transferred BALB/c cells. 5–10% of monocytes, all from the Gr-1^{hi} subset in CLL-treated mice, reacted specifically with the Y-Ae mAb (Fig. 7 B). The intensity with which these cells reacted with the Y-Ae mAb increased after the monocytes were cultured for 2 d in the presence of GM-CSF to induce CD11c and direct their differentiation toward a DC phenotype (Fig. 7 C; reference 32). The increased staining for Y-Ae on the cell surface of Y-Ae–positive monocytes indicates that a depot of antigen can be maintained intracellularly for up to 2 d and later presented more efficiently on the surface as differentiation proceeds.

Therefore, we investigated whether monocytes that phagocytize cell-associated antigens in the bone marrow would trigger T cell responses in the bone marrow or other lymphoid tissues. We measured the proliferation of CFSE-labeled OT-II T cells in which the TCR of $CD4^+$ cells is restricted to OVA peptide. We covalently coupled OVA protein to carboxylate-modified red fluorescent particles for delivery first to neutrophils and B cells, which, in turn, would transfer the particles to monocytes. Because the presentation of antigen by B cells themselves would confound our analysis, all experiments were performed in B cell–deficient μMT mice alongside WT mice. Red fluorescent particles (OVA coupled or plain) labeled monocytes just as well and as specifically as FITC-labeled LX particles used in the previous experiments (unpublished data).

Plain (no OVA) LX particles or OVA-coupled LX particles were injected in mice initially depleted of monocytes to set up labeling of Gr-1^{hi} monocytes by cell transfer. Particle-bearing monocytes were found to express I-A^b, which may become up-regulated in response to the particle itself. CFSE-labeled $CD4^+$ T cells from OT-II mice were injected i.v. 1 d later. 3 d after the adoptive transfer of T cells in OVA-coupled LX-treated mice, proliferation was evident among the OT-II T cells recovered from the blood, lymph nodes, and spleen but not from the bone marrow. Proliferation did not occur in mice that received plain (no OVA) LX particles (Fig. 8 A). Mice injected with OVA protein i.p. served as a positive control (not depicted).

When the same OVA-conjugated particles were engulfed by Gr-1^{lo} monocytes using the protocol shown in Fig. 1, OT-II T cell proliferation was evident when we sampled blood, lymph nodes, or spleen but not bone marrow. Thus, targeting of antigen to either monocyte subset led to the activation of antigen-specific T cell responses (representative data shown for the spleen in Fig. 8 B).

We wanted to be sure that T cell proliferation was caused by OVA antigen delivered to bone marrow monocytes that later matured to present the antigen in peripheral lymphoid tissues. Thus, we repeated experiments assessing T cell proliferation in mice that received adoptively transferred populations of monocytes that had engulfed LX^+ cells in the bone marrow. Bone marrow monocytes from mice injected with OVA-conjugated particles and CLLs were transferred into MHC-II–deficient recipients that had been preinjected with CFSE-labeled OT-II T cells. MHC-$II^{-/-}$ recipient mice were used to prevent cross-presentation from possibly dying transferred monocytes to the CD4 T cells. Proliferating T cells were evident 6 d later in lymphoid organs and blood (Fig. 8 C).

DISCUSSION

In this study, we report methods to selectively label mouse monocyte subsets by injecting particles for phagocytosis i.v. Under conditions in which particles are administered without further perturbations to the mouse, monocytes in the circulation are the major population labeled, where ~10% of monocytes in the blood engulf the microspheres. Initially, this fraction of labeled monocytes is comprised of both Gr-1^{hi} and Gr-1^{lo} monocyte subsets, but, within 24 h, all of the microsphere-bearing monocytes in the blood are part of the Gr-1^{lo} subset. Gr-1^{hi} monocytes serve as the precursors for Gr-1^{lo} monocytes (7, 26), but it remains unclear what events or molecules trigger the conversion from the Gr-1^{hi} to the Gr-1^{lo} phenotype. It appears that administration of the microspheres themselves promotes rapid conversion. A slower rate of conversion is observed when spontaneous conversion of Gr-1^{hi} monocytes is allowed to occur (e.g., after transient clodronate liposome-mediated depletion; references 7, 26).

The intention of developing this method was to apply the technique in tracing monocyte subset recruitment and differentiation. The administration of FITC-LX microspheres stably labeled only the Gr-1^{lo} monocytes, which limited the application of this technique to tracing only the fate of Gr-1^{lo} monocytes. However, we determined that the same

method—the injection of LX microspheres i.v.—could be used to selectively label blood Gr-1^{hi} monocytes when the administration of particles was coupled with protocols to deplete monocytes. In this case, the new monocytes that entered the circulation after their depletion are uniformly of the Gr-1^{hi} subset, and, again, at least 10% of them carried LX. Thus, these two protocols involving i.v. administration of LX microspheres permit distinct tracking of the fate of monocytes derived from different subsets over time. The technique is readily applicable to protocols that aim to trace the differentiation and migratory fate of monocytes in vivo, and we have already used the approach in a study that reveals that Gr-1^{hi} monocytes develop into Langerhans cells after skin injury (9). Importantly, phagocytosis of the labeled particles, at least in the small quantities that are taken up in our protocol, does not alter the trafficking capacity of the monocytes (unpublished data).

It was particularly unexpected that monocytes (Gr-1^{hi}) appeared in blood labeled with i.v.-administered microspheres under circumstances in which the particles were initially injected into mice that had been depleted of monocytes. As we explored how this labeling occurred, it became apparent that bone marrow monocytes (or promonocytes) were engulfing other cells, namely B cells and neutrophils, that carried the particles to the bone marrow in the first place. Indeed, although monocytes were the major cell type labeled with microspheres when they were injected into unperturbed mice, a substantial fraction of the label was also associated with various cells in the spleen that did not substantially partition in the blood: macrophages, neutrophils, and, surprisingly, marginal zone B cells. Macrophages and neutrophils clearly engulfed the microspheres they associated with, as these spheres were inaccessible to a mAb against FITC (the fluor incorporated in the microspheres) applied to the cell surface. In contrast, whereas B cells stably associated with particles and could carry them into distal locations like bone marrow and lymph nodes when they left the spleen, they failed to internalize the particles.

We observed that neutrophils and B cells were carrying the particles to the bone marrow and that detection of these cells with the particles dissipated at the same time we began to observe Gr-1^{hi} monocytes in the bone marrow that had internalized beads. As a result, we wondered whether the labeled monocytes may be engulfing the incoming neutrophils and B cells. Neutrophils that migrate to the bone marrow after having been in the periphery are typically senescent (17). Considering these recent findings, it was not surprising that the neutrophils likely die in the bone marrow. First, we wanted to be sure that acquisition of the particles required the migration of neutrophils and B cells to the bone marrow as opposed to other possibilities like accumulation of free beads in the bone marrow. Using the broadly effective inhibitor of migration PT, we observed that the labeling of bone marrow monocytes was greatly impeded in the presence of PT, indicating that the process by which the label was transferred was not passive, as would be the case with free beads. Adoptive transfer experiments furthermore illustrated that the transfer of congenic CD45.2$^+$ neutrophils or B cells bearing particles into CD45.1$^+$ hosts resulted in CD45.1$^+$ monocytes carrying particles in the circulation. Thus, there was a clear transfer of particles first borne by neutrophils or B cells into monocytes. Finally, the transfer of BALB/c B cells into C57BL/6 hosts revealed monocytes that carried an epitope derived from B cells and recognized by the Y-Ae mAb, indicating that more than just the particle was transferred to the monocytes. Indeed, some monocytes must be, to some extent, internalizing B cells themselves. However, we cannot eliminate the possibility (and indeed consider it likely) that some of the transferred particles are dropped from the surface of B cells after their arrival in the bone marrow and are engulfed by the monocytes thereafter. A similar outcome of robust monocyte labeling occurs in the absence of B cells (μMT mice) when neutrophils are the major transferring cell, and because the neutrophils fully phagocytize the particles, it is very likely that in this scenario monocytes acquire the particles essentially completely through the uptake of senescent neutrophils.

Considering that neutrophils, but not B cells, internalized the particles and that neutrophils are known to die in the bone marrow (17), the observation that neutrophils transfer antigens to monocytes is likely more physiologically relevant than the transfer of particles by marginal zone B cells. Nonetheless, it is likely that any cell that dies in the bone marrow, either after developing in the bone marrow or after migrating there, could be acquired by monocytes as shown herein for the labeled cells that we trace. It is becoming increasingly clear that a range of leukocytes migrate from blood back to bone marrow under certain circumstances (33).

The sequence of events that leads to the spread of infection with *Listeria monocytogenes* is becoming increasingly clear, and several steps in the spread of infection are strikingly reminiscent of our observations. First, *L. monocytogenes* that initially gain access to the bloodstream primarily accumulate in the liver (34). Neutrophils attracted by inflammatory signals enter the liver and become the major cell type initially involved in killing *L. monocytogenes* (34) because, at least in mice, *L. monocytogenes* are found to be adherent to the surface of Kupffer cells rather than inside them (34). Later, the bone marrow becomes a major reservoir for the bacteria, and there they grow within cells that have the same phenotype of the immature monocytes that acquire particles in the bone marrow (35). Any senescent neutrophils that home to the bone marrow (17) from the liver may harbor a few live rather than killed bacteria and efficiently transfer them to monocytes in accordance with our observations. These monocytes, after entering the blood, act as Trojan horses to transport the bacteria to distal sites like the central nervous system (8, 34–36), where they can cause meningitis. Our findings indicate that bone marrow monocytes may pick phagocytic material in the bone marrow routinely, so the fact that they pick up *L. monocytogenes* and transport it distally is not unique to *L. monocytogenes* infection. Indeed, this property may extend

to a variety of other infections. Neutrophils also play an important role in serving as a medium for the cross-presentation of *L. monocytogenes* antigens by DCs (37), fitting with the possibility that some monocytes that took up neutrophils in the bone marrow carrying killed bacteria may have differentiated to DCs with the capacity to present these antigens to peripheral T cells.

Indeed, in our study, we found that monocytes were capable of processing and presenting antigens transferred from B cells and neutrophils. The presentation did not take place in the bone marrow, which is in contrast to presentation that occurs in response to splenic DCs that emigrate from the blood to the bone marrow (33). Instead, we found that after mobilizing from the bone marrow, monocytes express evidence on their surface of having engulfed, processed, and presented epitopes from adoptively transferred B cells. The intensity of this MHC-II presentation increases when the monocytes are kept in culture for 2 d in the presence of GM-CSF to promote their differentiation toward DCs (32), indicating that the monocytes retained a pool of foreign antigens intracellularly for presentation later as they augmented their phenotype and shifted toward DCs. T cell proliferation was detectable in vivo a few days after transferring bone marrow–derived monocytes to the skin that had engulfed OVA-LX$^+$ cells in the bone marrow before transfer. Some of these monocytes migrated from the skin to the draining lymph nodes, and T cell proliferation was induced. Thus, these data indicate that the handling of antigen by monocytes does not mirror the proteolytically destructive nature of macrophages toward engulfed antigens (21) such that when some monocytes differentiate to DCs a few days after leaving the bone marrow, they are able to "recall" previously engulfed antigens for presentation.

MATERIALS AND METHODS

Mice. C57BL/6, congenic Ly5.1 (CD45.1) C57BL/6, BALB/c, and B cell–deficient μMT mice were purchased from The Jackson Laboratory. OT-II and MHC-II$^{-/-}$ mice were maintained in our colony. All mice were housed in a pathogen-free environment. All experiments were performed with age- and sex-matched animals at 6–12 wk of age in accordance with the Institutional Animal Care and Utilization Committee's (Mount Sinai School of Medicine) approved protocols.

Labeling of blood monocytes. 0.5-μm FITC-conjugated (yellow gold) plain microspheres (2.5% solids [wt/vol]; Polysciences, Inc.) were diluted 1:25 in PBS, and 250 μl of the solution was injected into the lateral tail vein for labeling of Gr-1^{lo} monocytes. For labeling of Gr-1^{hi} monocytes, 250 μl of liposomes containing clodronate were i.v. injected followed by 250 μl of fluorescent microspheres i.v. 16–18 h later. Clodronate was a gift from Roche and was incorporated into liposomes as previously described (27). We used the dose of CLL shown to fully eliminate blood monocytes (26); this method, with the introduction of CLL i.v., will also eliminate splenic and liver macrophages (27). Other macrophage populations are protected because CLL will not cross vascular barriers (27). In some experiments, red fluorescent (580-nm excitation wavelength and 605-nm emission wavelength) carboxylate-modified 0.5-μm microspheres (2.0% solids [wt/vol]; Invitrogen) were used and conjugated to OVA (Sigma-Aldrich). Coupling of OVA to these particles was performed using the Carbodiimide Kit from Polysciences, Inc.

Analysis of blood and tissues. Whole blood was drawn and subjected to red cell lysis using Pharmlyse (BD Biosciences), washed twice with DME containing 5 mM EDTA and 0.5% BSA, and stained with antibodies for FACS analysis. For flow cytometric analysis of tissues, lymph nodes (brachial, axillary, cervical, popliteal, and inguinal) or spleen were dissociated into single-cell suspensions with collagenase D (Roche) for 30 min at 37°C. Back skin was excised and digested using Liberase III (Roche) as described previously (7). Bone marrow cells were obtained by flushing the femur and tibia with HBSS containing 0.1% BSA and 5 mM EDTA followed by red blood lysis and two washes in HBSS. For immunohistochemistry, fresh tissues were frozen directly with Tissue Tek optimal cutting temperature (Sakura Finetek). Sections of 8-μm thickness were cut using a cryomicrotome (1900CM; Leica) and fixed with 3% paraformaldehyde on polylysine-coated slides.

Flow cytometry. Four-color staining for flow cytometric analysis was conducted using combinations of the following mAbs. All mAbs to the following molecules were obtained from BD Biosciences except where otherwise indicated: F4/80 (Serotec), CD115 (eBioscience), CD4 (eBioscience), CD11c (eBioscience), CD45.1 (eBioscience), CD45.2 (eBioscience), anti-FITC (Jackson ImmunoResearch Laboratories), Gr-1, CD11b, IA^b, B220, CD19, NK1.1, DX5, CD8, CD3, CD62L, mouse IgG1, rat IgG2a, and hamster IgG isotype controls. Biotinylated annexin V (Sigma-Aldrich) was used to identify apoptotic cells followed by streptavidin-APC (Caltag) incubation. Flow cytometric analysis was performed on a FACScalibur (BD Biosciences) and analyzed with FlowJo software (Tree Star).

Immunohistochemistry. Immunofluorescence microscopy was performed using biotin-conjugated CD11b or rat IgG (BD Biosciences) and streptavidin-Cy3 (Sigma-Aldrich). Slides were mounted with Vectashield containing DAPI (Vector Laboratories). Images were acquired using a fluorescence microscope (DMRA2; Leica) and a digital CCD camera (model ORCA-ER; Hamamatsu) and were analyzed using Openlab software (Improvision).

Blockage of cell homing to bone marrow. Mice were injected i.v. with LX particles followed by CLL 8–10 h later. At the time of liposome injection, mice received either PBS or 400 ng PT i.v. (List Biological Laboratories). PT, an exotoxin produced by Bordetella pertussis, blocks the signaling through G_i protein–coupled receptors by mediating adenosine diphosphate ribosylation of their α subunits (38, 39). Results were analyzed after 16 h. To ensure that PT did not impair the phagocytic capacity of monocytes, mice received either PBS or 400 ng PT i.v. followed by 250 μl of 0.5-μm LX beads (diluted 1:25) i.v. 2 h later (as described for Gr-1^{lo} monocyte labeling). Blood, spleen, and bone marrow cells were analyzed 4 and 24 h thereafter.

Adoptive transfer of LX$^+$ B cells and neutrophils. To label B cells with LX microspheres, C57BL/6 mice were injected with 250 μl CLL i.v. followed by 250 μl of 0.5-μm LX beads diluted 1:25 i.v. 18 h later (as described for Gr-1^{hi} monocyte labeling). 4 h later, CD45.2$^+$ B cells were isolated from the spleen by positive magnetic cell separation using anti-B220 microbeads (Miltenyi Biotec) with a purity of 95–98%, and 15–20% of these cells were LX$^+$. 10 million cells were injected into monocyte-depleted (18 h after clodronate liposomes i.v.) CD45.1$^+$ mice corresponding to ~1.5–2 × 10^6 LX$^+$ B cells per recipient mouse.

For ex vivo labeling of neutrophils, bone marrow was flushed from CD45.2$^+$ mice, washed, and whole bone marrow cells were incubated with LX beads in RPMI-1640 containing 50% FBS at 37°C for 1 h. The majority of isolated bone marrow cells were neutrophils (17), and 75% of the LX$^+$ cells were neutrophils. 27 million of these cells were injected into monocyte-depleted (18 h after the administration of CLL i.v.) CD45.1$^+$ mice, corresponding to 6 × 10^6 LX$^+$ cells per animal. The neutrophil phenotype was confirmed by staining for CD11b and Gr-1 and typical multilobulated nuclear morphology in cytocentrifuge preparations.

Analysis of antigen presentation. BALB/c B cells were isolated from spleen and lymph nodes by positive magnetic cell separation using B220 microbeads (Miltenyi Biotec) with a purity of 95–98%. 5×10^6 $B220^+$ BALB/c cells were injected i.v. per mouse into clodronate liposome–treated C57BL/6 mice 18 h after liposome injection. Blood cells of recipient mice were analyzed 1 or 3 d after B cell transfer. To directly assess antigen presentation, we used biotin-conjugated Y-Ae antibody that recognizes I-Eα 56–73 peptide from BALB/c donor cells in the context of C57BL/6 recipient I-A^b molecules (31). Streptavidin-APC (Caltag) was used for detection. Blood monocytes were obtained 3 d after BALB/c B cell transfer or from untreated controls and were cultured for 2 d in RPMI-1640 with 10% FBS, penicillin/streptomycin, and 5×10^{-5} M β-mercaptoethanol. The cultures were supplemented with GM-CSF contained in the supernatant of J5587 cells to promote differentiation toward a DC phenotype as described previously (32). I-A^d staining (BD Biosciences) was used to monitor the presence of live BALB/c B cells (100% positive).

T cell proliferation assays. $CD4^+$ T cells were isolated from spleen and lymph nodes of OT-II mice using CD4 microbeads (Miltenyi Biotec). OT-II cells were labeled with 5-CFSE (Invitrogen) by incubation with 5 μM CFSE in RPMI-1640 for 10 min, and $1–2 \times 10^6$ $CD4^+$ $CFSE^+$ OT-II cells were injected per animal. C57BL/6 WT or μMT mice received i.v. either plain red fluorescent beads or red fluorescent OVA-coupled beads. Some of these mice received CLLs 18 h before LX was administered. 1 d later, $CD4^+$ $CFSE^+$ OT-II cells were injected i.v., and T cell proliferation monitored by CFSE dye dilution was analyzed 3 d later in blood, lymph nodes, spleen, and bone marrow.

Adoptive monocyte transfer to test T cell proliferation. To label monocytes with OVA-coupled particles, C57BL/6 mice were injected with red fluorescent OVA-coupled beads and with CLL 8 h later. 16 h thereafter, mice were killed, and bone marrow monocytes were isolated by positive magnetic cell separation using biotin-conjugated CD115 (eBioscience) followed by streptavidin-coupled microbeads (Miltenyi Biotec), yielding a purity of 95–98%. 15–30% of the isolated monocytes also carried microspheres. To exclude cross-presentation of dying monocytes after adoptive transfer, the recipients of adoptively transferred monocytes were MHC-$II^{-/-}$ mice. T cells were isolated from spleen and lymph nodes of OT-II mice, labeled with CFSE ex vivo, and injected i.v. (10×10^6 total cells per animal, corresponding to $1–2 \times 10^6$ $CD4^+$ $CFSE^+$ cells) into MHC-$II^{-/-}$ mice. 1 d later, $3–5 \times 10^6$ bone marrow monocytes or $6–10 \times 10^6$ OVA-loaded spleen DCs used as a positive control were intradermally injected into the shaved back skin and front footpad (25, 32). Mice were killed after 3 or 6 d; lymph nodes, spleen, blood, and skin were analyzed for the presence of particle-bearing cells and T cell proliferation (CFSE dye dilution).

Online supplemental material. Fig. S1 shows that beads administered i.v. are acquired almost in total by cells and that few free beads remain in the blood or enter the bone marrow. Online supplemental material is available at http://www.jem.org/cgi/content/full/jem.20052119/DC1.

This work was supported by the National Institutes of Health (NIH) grant AI49653 to G.J. Randolph, a postdoctoral fellowship from the German Research Foundation to F. Tacke, and a NIH training grant to C. Jakubzick.

The authors have no conflicting financial interests.

Submitted: 20 October 2005
Accepted: 26 January 2006

REFERENCES

1. Gordon, S. 1986. Biology of the macrophage. *J. Cell Sci. Suppl.* 4:267–286.
2. Ziegler-Heitbrock, H.W. 1989. The biology of the monocyte system. *Eur. J. Cell Biol.* 49:1–12.
3. Imhof, B.A., and M. Aurrand-Lions. 2004. Adhesion mechanisms regulating the migration of monocytes. *Nat. Rev. Immunol.* 4:432–444.
4. Leon, B., M. Lopez-Bravo, and C. Ardavin. 2005. Monocyte-derived dendritic cells. *Semin. Immunol.* 17:313–318.
5. Randolph, G.J., G. Sanchez-Schmitz, R.M. Liebman, and K. Schakel. 2002. The CD16(+) (FcγRIII(+)) subset of human monocytes preferentially becomes migratory dendritic cells in a model tissue setting. *J. Exp. Med.* 196:517–527.
6. Geissmann, F., S. Jung, and D.R. Littman. 2003. Blood monocytes consist of two principal subsets with distinct migratory properties. *Immunity.* 19:71–82.
7. Qu, C., E.W. Edwards, F. Tacke, V. Angeli, J. Llodra, G. Sanchez-Schmitz, A. Garin, N.S. Haque, W. Peters, N. van Rooijen, et al. 2004. Role of CCR8 and other chemokine pathways in the migration of monocyte-derived dendritic cells to lymph nodes. *J. Exp. Med.* 200:1231–1241.
8. Drevets, D.A., M.J. Dillon, J.S. Schawang, N. Van Rooijen, J. Ehrchen, C. Sunderkotter, and P.J. Leenen. 2004. The Ly-6Chigh monocyte subpopulation transports *Listeria monocytogenes* into the brain during systemic infection of mice. *J. Immunol.* 172:4418–4424.
9. Ginhoux, F., F. Tacke, V. Angeli, M. Bogunovic, M. Loubeau, X.M. Dai, E.R. Stanley, G.J. Randolph, and M. Merad. 2006. Langerhans cells arise from monocytes in vivo. *Nat. Immunol.* doi:10.1038/ni1307.
10. Savill, J., V. Fadok, P. Henson, and C. Haslett. 1993. Phagocyte recognition of cells undergoing apoptosis. *Immunol. Today.* 14:131–136.
11. Savill, J., I. Dransfield, C. Gregory, and C. Haslett. 2002. A blast from the past: clearance of apoptotic cells regulates immune responses. *Nat. Rev. Immunol.* 2:965–975.
12. Newman, S.L., J.E. Henson, and P.M. Henson. 1982. Phagocytosis of senescent neutrophils by human monocyte-derived macrophages and rabbit inflammatory macrophages. *J. Exp. Med.* 156:430–442.
13. Savill, J., I. Dransfield, N. Hogg, and C. Haslett. 1990. Vitronectin receptor-mediated phagocytosis of cells undergoing apoptosis. *Nature.* 343:170–173.
14. Savill, J. 1997. Recognition and phagocytosis of cells undergoing apoptosis. *Br. Med. Bull.* 53:491–508.
15. Ren, Y., and J. Savill. 1995. Proinflammatory cytokines potentiate thrombospondin-mediated phagocytosis of neutrophils undergoing apoptosis. *J. Immunol.* 154:2366–2374.
16. Dogusan, Z., E. Montecino-Rodriguez, and K. Dorshkind. 2004. Macrophages and stromal cells phagocytose apoptotic bone marrow-derived B lineage cells. *J. Immunol.* 172:4717–4723.
17. Martin, C., P.C. Burdon, G. Bridger, J.C. Gutierrez-Ramos, T.J. Williams, and S.M. Rankin. 2003. Chemokines acting via CXCR2 and CXCR4 control the release of neutrophils from the bone marrow and their return following senescence. *Immunity.* 19:583–593.
18. Jung, S., D. Unutmaz, P. Wong, G. Sano, K. De los Santos, T. Sparwasser, S. Wu, S. Vuthoori, K. Ko, F. Zavala, et al. 2002. In vivo depletion of CD11c(+) dendritic cells abrogates priming of CD8(+) T cells by exogenous cell-associated antigens. *Immunity.* 17:211–220.
19. Inaba, K., S. Turley, F. Yamaide, T. Iyoda, K. Mahnke, M. Inaba, M. Pack, M. Subklewe, B. Sauter, D. Sheff, et al. 1998. Efficient presentation of phagocytosed cellular fragments on the major histocompatibility complex class II products of dendritic cells. *J. Exp. Med.* 188:2163–2173.
20. Liu, K., T. Iyoda, M. Saternus, Y. Kimura, K. Inaba, and R.M. Steinman. 2002. Immune tolerance after delivery of dying cells to dendritic cells in situ. *J. Exp. Med.* 196:1091–1097.
21. Delamarre, L., M. Pack, H. Chang, I. Mellman, and E.S. Trombetta. 2005. Differential lysosomal proteolysis in antigen-presenting cells determines antigen fate. *Science.* 307:1630–1634.
22. Inaba, K., S. Turley, T. Iyoda, F. Yamaide, S. Shimoyama, C. Reise e Sousa, R.N. Germain, I. Mellman, and R.M. Steinman. 2000. The formation of immunogenic major histocompatibility complex class II-peptide ligands in lysosomal compartments of dendritic cells is regulated by inflammatory stimuli. *J. Exp. Med.* 191:927–936.
23. Schmid, H., R. Sauerbrei, G. Schwarz, E. Weber, H. Kalbacher, and C. Driessen. 2002. Modulation of the endosomal and lysosomal distribution of cathepsins B, L and S in human monocytes/macrophages. *Biol. Chem.* 383:1277–1283.

24. Authier, F., B.I. Posner, and J.J. Bergeron. 1996. Endosomal proteolysis of internalized proteins. *FEBS Lett.* 389:55–60.
25. Randolph, G.J., K. Inaba, D.F. Robbiani, R.M. Steinman, and W.A. Muller. 1999. Differentiation of phagocytic monocytes into lymph node dendritic cells in vivo. *Immunity.* 11:753–761.
26. Sunderkotter, C., T. Nikolic, M.J. Dillon, N. Van Rooijen, M. Stehling, D.A. Drevets, and P.J. Leenen. 2004. Subpopulations of mouse blood monocytes differ in maturation stage and inflammatory response. *J. Immunol.* 172:4410–4417.
27. Van Rooijen, N., and A. Sanders. 1994. Liposome mediated depletion of macrophages: mechanism of action, preparation of liposomes and applications. *J. Immunol. Methods.* 174:83–93.
28. Leenen, P.J., K. Radosevic, J.S. Voerman, B. Salomon, N. van Rooijen, D. Klatzmann, and W. van Ewijk. 1998. Heterogeneity of mouse spleen dendritic cells: in vivo phagocytic activity, expression of macrophage markers, and subpopulation turnover. *J. Immunol.* 160:2166–2173.
29. Karlsson, M.C., R. Guinamard, S. Bolland, M. Sankala, R.M. Steinman, and J.V. Ravetch. 2003. Macrophages control the retention and trafficking of B lymphocytes in the splenic marginal zone. *J. Exp. Med.* 198:333–340.
30. Cyster, J.G. 2003. Homing of antibody secreting cells. *Immunol. Rev.* 194:48–60.
31. Rudensky, A., S. Rath, P. Preston-Hurlburt, D.B. Murphy, and C.A. Janeway Jr. 1991. On the complexity of self. *Nature.* 353:660–662.
32. Rotta, G., E.W. Edwards, S. Sangaletti, C. Bennett, S. Ronzoni, M.P. Colombo, R.M. Steinman, G.J. Randolph, and M. Rescigno. 2003. Lipopolysaccharide or whole bacteria block the conversion of inflammatory monocytes into dendritic cells in vivo. *J. Exp. Med.* 198:1253–1263.
33. Cavanagh, L.L., R. Bonasio, I.B. Mazo, C. Halin, G. Cheng, A.W. van der Velden, A. Cariappa, C. Chase, P. Russell, M.N. Starnbach, et al. 2005. Activation of bone marrow-resident memory T cells by circulating, antigen-bearing dendritic cells. *Nat. Immunol.* 6:1029–1037.
34. Wing, E.J., and S.H. Gregory. 2002. *Listeria monocytogenes*: clinical and experimental update. *J. Infect. Dis.* 185:S18–S24.
35. Join-Lambert, O.F., S. Ezine, A. Le Monnier, F. Jaubert, M. Okabe, P. Berche, and S. Kayal. 2005. *Listeria monocytogenes*-infected bone marrow myeloid cells promote bacterial invasion of the central nervous system. *Cell. Microbiol.* 7:167–180.
36. Drevets, D.A., P.J. Leenen, and R.A. Greenfield. 2004. Invasion of the central nervous system by intracellular bacteria. *Clin. Microbiol. Rev.* 17:323–347.
37. Tvinnereim, A.R., S.E. Hamilton, and J.T. Harty. 2004. Neutrophil involvement in cross-priming CD8+ T cell responses to bacterial antigens. *J. Immunol.* 173:1994–2002.
38. Kaslow, H.R., and D.L. Burns. 1992. Pertussis toxin and target eukaryotic cells: binding, entry, and activation. *FASEB J.* 6:2684–2690.
39. He, J., S. Gurunathan, A. Iwasaki, B. Ash-Shaheed, and B.L. Kelsall. 2000. Primary role for Gi protein signaling in the regulation of interleukin 12 production and the induction of T helper cell type 1 responses. *J. Exp. Med.* 191:1605–1610.